TECHNICAL TRANSACTIONS | CZASOPISMO TECHNICZNE
CHEMISTRY | CHEMIA
2-Ch/2014

BOHUŠ KYSELA*, IVAN FOŘT**, JIŘI KONFRŠT*

CFD SIMULATION OF TURBULENT VELOCITY FIELD IN THE DISCHARGE STREEM FROM A STANDARD RUSHTON TURBINE IMPELLER

SYMULACJA KOMPUTEROWA (CFD) BURZLIWEGO POLA PRĘDKOŚCI W STRUMIENIU WLOTOWYM ZE STANDARDOWEJ TURBINY RUSHTONA

Abstract

The velocity field around the standard Rushton turbine was investigated by the Computational Fluid Dynamics (CFD) calculations and compared with results obtained from the Laser Doppler Anemometry (LDA) measured in a pilot plant baffled cylindrical vessel. For calculations the Large Eddy Simulation (LES) approach was employed. The impeller motion was modeled using the Sliding Mesh technique (SM). The mean ensemble-averaged velocity profiles and root mean square values of fluctuations were compared in the radial discharge jet from the standard Rushton turbine under turbulent regime of flow of agitated liquid. There were found two subregions in the discharge stream and the values of the axial profiles of the radial component of the fluctuating velocity are rather same determined from the LES calculations and from the LDA measurements in the second one ZEF (zone of established flow) of the impeller discharge stream, but they differ in the first region ZFE (zone of flow establishment) in the impeller vicinity, although they exhibit the same shape. The impeller power number derived from calculations shows also good agreement with values introduced in literature with a significant influence of the thickness of the impeller disc.

Keywords: *Rushton turbine*, *mixing*, *CFD*, *LES*, *LDA/LDV*, *agitated vessel*

Streszczenie

Pole prędkości wokół standardowej turbiny Rushtona przeanalizowano metodą CFD (Computer Fluid Dynamics) i porównano z wynikami uzyskanymi za pomocą laserowej anemometrii dopplerowskiej (LDA) w doświadczalnym zbiorniku cylindrycznym z przegrodami. W obliczeniach wykorzystano technikę LES (Large Eddy Simulation). Ruch mieszadła zamodelowano z zastosowaniem techniki SM (Sliding Mesh). Średnie ważone profile prędkości i średnie kwadratowe wartości fluktuacji porównano z promieniowym strumieniem cieczy wypływającej z turbiny Rushtona w warunkach burzliwego przepływu cieczy mieszanej. W strumieniu wypływającym z mieszadła wyodrębniono dwa podobszary, a przebiegi profili promieniowych składowych fluktuacji prędkości były zbliżone, zarówno otrzymane w wyniku obliczeń LES, jak i z pomiarów LDA w drugiej strefie przepływu ustabilizowanego w sąsiedztwie wirnika, chociaż wykazywały ten sam kształt. Liczba mocy mieszadła, otrzymana w wyniku obliczeń, wykazała dobrą zgodność z wartościami podawanymi w literaturze, przy znaczącym wpływie grubości tarczy mieszadła.

Słowa kluczowe: *turbina Rushtona*, *mieszanie*, *CFD*, *LES*, *LDA/LDV*, *mieszalnik*

* Ph.D. Ing. Bohuš Kysela, Ph.D. Ing. Jiří Konfršt, Institute of Hydrodynamics AS CR, Prague, Czech Republic.

** Ivan Fořt, Department of Process Engineering, Faculty of Mechanical Engineering, Czech Technical University in Prague, Czech Republic.

Nomenclature

b – width of radial baffle [m]
C – impeller off-bottom clearance [m]
D – impeller diameter [m]
H – height of agitated charge above vessel bottom [m]
h – impeller blade width [m]
M_k – impeller torque [Nm]
N – number of experimental points
n – impeller speed [s^{-1}]
Po – impeller power number
r – dimensional longitudinal (radial) coordinate [m]
r^* – dimensionless longitudinal (radial) coordinate
Re_M – impeller Reynolds number $\mathrm{Re}_M = nD^2\rho/\mu$
t – thickness of the impeller separating disc [m]
T – mixing vessel diameter [m]
V_{tip} – impeller tip speed [$m \cdot s^{-1}$]
W_r^* – dimensionless radial ensemble-averaged mean velocity
w_r' – dimensionless root mean square value of the radial component of fluctuating velocity

Greek symbols

μ – dynamic viscosity [Pa·s]
ρ – density [$kg \cdot m^{-3}$]
σ – standard deviation

1. Introduction

The flow inside the agitated vessel has a key role in the mixing processes. Only the CFD modeling gives us the complex information about the whole flow field in contrary with the results of the experimental measurements. The enormous progress of the computational equipment has allowed using more exacting turbulence models for solution of the flow in the agitated vessel. Nowadays not only Reynolds Averaged Navier-Stokes (RANS) models, e.g. k–ε [1–6], k–ε, Reynolds Stress Model (RSM) [3, 4] are commonly used, but also other more sophisticated methods become topical, e.g. Detached Eddy Simulation (DES) [7], Large Eddy Simulation (LES) [7–14] and even Direct Numerical Simulation (DNS) [14]. However, all calculations also need some validation by the experimental results or by the analytical models. The radial impellers are most often used in experiments and calculations [15–20], namely Rushton turbine and there are also analytical models, where the impeller discharge stream is modeled as a turbulent jet [1, 15, 18, 19].

The aim of this study is the description of the turbulent velocity field in the discharge stream from the standard Rushton turbine impeller in the pilot plant mixing vessel with baffles at the wall. Investigation will be carried out experimentally (LDA technique) as well as by means of CFD simulation, where the LES approach was used with (SM) technique for the impeller movement, because this approach has a potential to be used as a design tool to screen different configurations, but it has not been sufficiently validated for turbulent regime [4].

2. CFD calculations

A commercial ANSYS FLUENT v.13.0 solver of the finite volume method was employed. The turbulence was modelled by Large Eddy Simulation (LES) with Sliding Mesh (SM) simulation for the impeller movement. The solver was pressure based and for pressure-velocity coupling the PISO method was used. The subgrid-scale model was used Smagorinsky-Lilly with Second Order Implicit scheme. The schemes for spatial discretization were: Gradient – Least Squares Cell based, Pressure – Second Order, and Momentum, was Second Order Upwind. The boundary conditions were set: water level to the symmetry and others to the no slip wall, where the part of the impeller shaft outside of the sliding region is defined as wall with impeller speed velocity. The walls of the vessel and baffles are provided by the boundary layer mesh see Fig. 1. The sliding region has cylindrical shape with distance D/10 from the impeller cylindrical envelope see Fig. 2. The solved hexahedral meshes consists of 2 465 228 cells (LES 1) and 7 435 557 cells (LES 2), respectively. The finer mesh was refined namely in bulk vessel region to attained the maximal cell size under 2 mm, which corresponds with maximal size of the measurement LDA volume, see section experimental. The time step must not exceed 1/60 of one revolution [10] that corresponds with 0.0032 s for 300 rpm. Hence, the time step was determined 0.001 s. The calculated time was 60 s while the flow development required min 20 revolutions [7, 12] which represent the first 2 s of the simulation. Calculated instantaneous flow field over 60 s in the measured plane is depicted in Fig. 3. The instantaneous calculated values were time averaged last 30 s of calculations and the ensemble-averaged values were obtained in the proposed axial profiles.

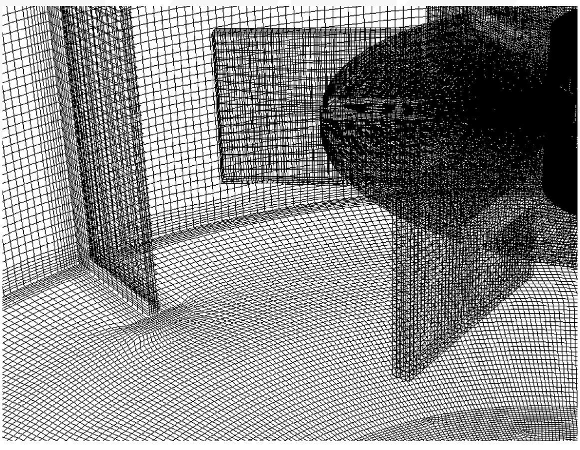

Fig. 1. Mesh in the baffles vicinity and on the impeller surface in detail (LES 1)

Fig. 2. Mesh (LES 1) on the vessel wall and impeller with the highlighted sliding region around the impeller

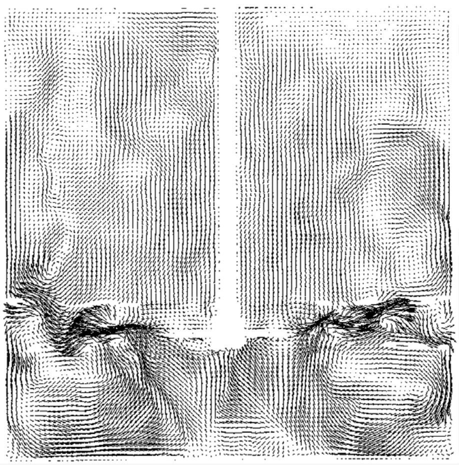

Fig. 3. Calculated instantaneous flow field in measured plane between the baffles

3. Experimental

Measurements of the velocity profiles were carried out in a pilot plant flat bottomed mixing vessel with four baffles at its wall (see Fig. 4), with water as the working liquid (density $\rho = 1000$ kg m^{-3}, dynamic viscosity $\mu = 1$ mPa s) under the constant impeller speed 300 rpm (Impeller Reynolds number $Re_M = 50\ 000$). A standard Rushton impeller [21, 22] was used for the investigation (Fig. 5).

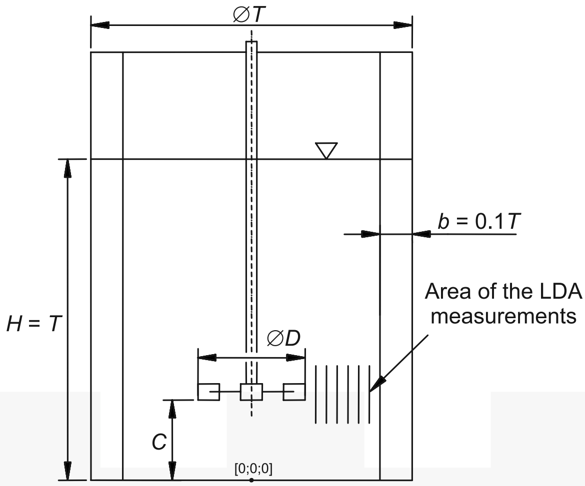

Fig. 4. Pilot plant cylindrical vessel with a six-blade Rushton turbine (T = 300 mm, H/T = 1, D/T = 1/3, C/D = 0.75, b/T = 1/10, four baffles)

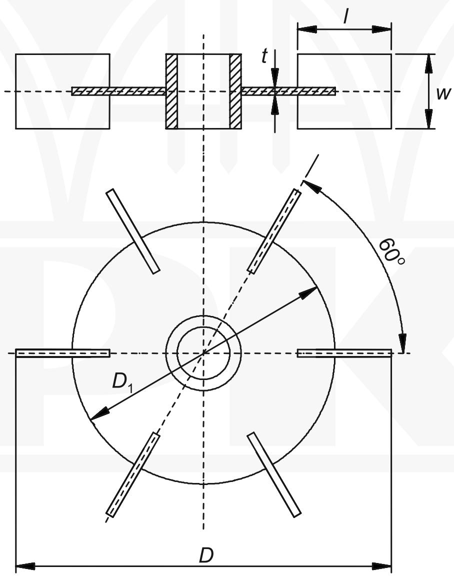

Fig. 5. Sketch of Rushton turbine impeller w/D = 0.2, D_l/D = 0.75, l/D = 0.25

Laser Doppler Anemometry (LDA) one component measurements (in back scattering mode) of the radial velocity were performed in the impeller discharge stream (see Fig. 4.) in the vertical plane between two adjacent baffles in axial profiles with several distances from the impeller blade. The dimensionless radial coordinates $r^* = 2r/D$ were: 1.2; 1.4; 1.6; 1.8; 2.0; 2.2. One component LDA system set-up consists of: Coherent INNOVA 305

Ion-Argon laser supply with power 5 W and separated beam only for one component measurement on wavelength 514.5 nm; DANTEC fiberflow transmitting optics and P80 DANTEC BSA processor. The optic parameters were: focal length 310 mm, diameter of the beam 1.2 mm, fringe spacing 2.67 μm, number of fringes 63, and the measured volume was ellipsoid with sizes of the axes 0.170 × 0.169 × 1.757 mm. The used frequency shift was 40 MHz, and velocity span 7.51 m/s. The set-up was supervised by BSA FLOW SOFTWARE v3.0 installed on standard PC where the data was processed. S-HGS (Silver coated – Hollow Glass Spheres) with mean diameter 10 μm and density 1.1 g·cm^{-3} were used as trace particles. The measurement was performed through the glass flat bottom of the vessel to eliminate optical effects of the cylindrical walls.

4. Results and discussion

Profiles of the radial mean ensemble-averaged velocity component in the dimensionless form where the radial velocity component is normalized by the impeller tip speed $V_{tip} = \pi Dn$ are depicted in Figs. 6–11. The dimensionless coordinate z^* is the distance from the impeller

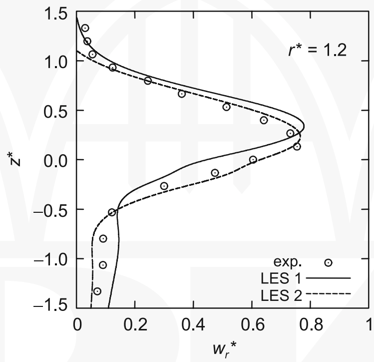

Fig. 6. Radial component of the ensemble-averaged mean velocity at $r^* = 1.2$

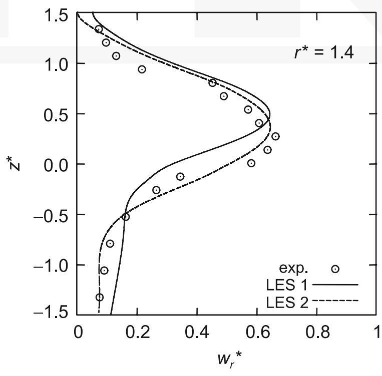

Fig. 7. Radial component of the ensemble-averaged mean velocity at $r^* = 1.4$

disk axis normalized by the half-height of the impeller blade $w/2$. The profiles are depicted for six values of the dimensionless radius r^*.

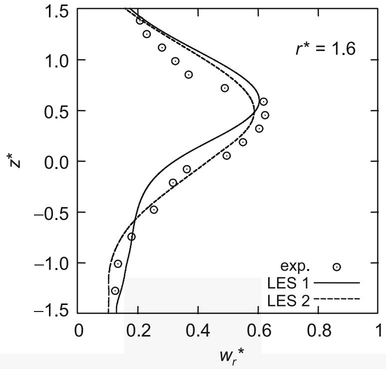

Fig. 8. Radial component of the ensemble-averaged mean velocity at $r^* = 1.6$

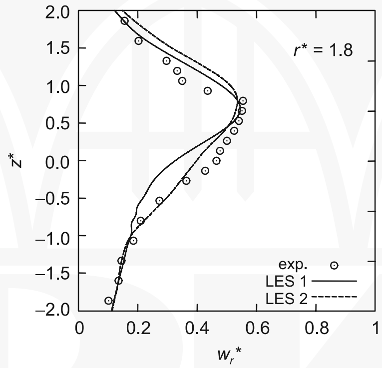

Fig. 9. Radial component of the ensemble-averaged mean velocity at $r^* = 1.8$

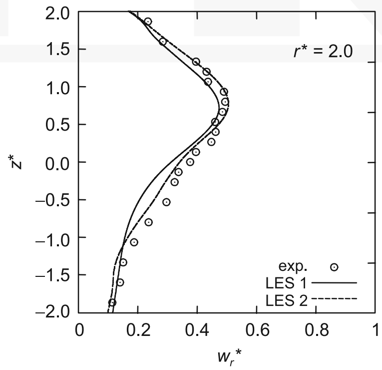

Fig. 10. Radial component of the ensemble-averaged mean velocity at $r^* = 2.0$

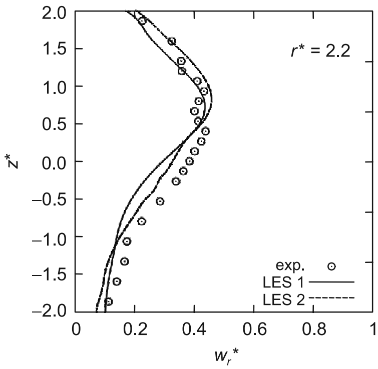

Fig. 11. Radial component of the ensemble-averaged mean velocity at r^* = 2.2

The depicted results from CFD calculations and results in measured points were quantitatively compared by calculations of the mean square difference, i.e. the difference between the measured and the calculated data of dimensionless radial component of the mean ensemble-averaged velocity. It was calculated using formula:

$$\mathrm{var}\,(W_r^*) = \frac{1}{N}\sum_{i=1}^{N}(W_{r\mathrm{LDA}}^* - W_{r\mathrm{CFD}}^*)^2, \tag{1}$$

where N = 24 is number of compared points on the profile, W_r^* with index LDA means the value obtained from LDA measurements and with index CFD it is the value interpolated from calculated profile from CFD. Root mean square difference σ is expressed as the square root of quantity $\mathrm{var}\,(W_r^*)$. The results of mean square difference in Tab. 1 signify that the higher discrepancy of the profiles is in the region where the zone of establishment is changing to the zone of the established flow [1]. The increase of the standard deviation with increasing dimensionless radius is probably caused by the different shape of the discharge stream and it seems to be different also at the vertical position of the stream which depends on the impeller off-bottom clearance. Comparison results in Table 1 for simulation LES 1 and LES 2 supports an idea to use a finer mesh for CFD simulation.

Table 1

Values of the mean square difference among LDA data of the mean ensemble-averaged radial velocity component and profiles obtained from CFD in dimensionless form

	LES 1		LES 2	
r^*	var (W_r^*)	σ	var (W_r^*)	σ
1.2	0.0055	0.074	0.0017	0.042
1.4	0.0082	0.090	0.0026	0.051
1.6	0.0056	0.075	0.0024	0.049
1.8	0.0042	0.065	0.0032	0.057
2.0	0.0017	0.042	0.0006	0.024
2.2	0.0027	0.052	0.0017	0.041

The r.m.s values of the fluctuation velocity were treated as well as the mean velocities to the dimensionless form. The two values of the dimensionless radius r^* = 1.4 and 1.6 are shown in Fig. 12, where the trailing vortices have an impact to the fluctuation velocity. The zone is titled the zone of flow establishment (ZFE) [1]. The calculated values of the fluctuations are rather lower than the measured ones. The results in the next zone titled the zone of established flow (ZEF) are depicted in Fig. 13. There are compared values of the dimensionless radius r^* = 2.0 and 2.2. It seems that agreement between computed and experimentally determined values of the fluctuating velocity is better in ZEF than in ZFE, because of no contribution of the periodic part of turbulence (pseudoturbulence) to the fluctuation velocity component in this part of the impeller discharge stream.

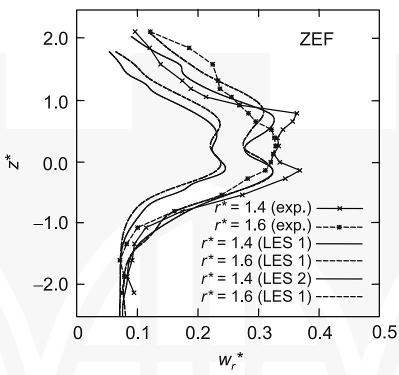

Fig. 12. Comparison of axial profiles of r.m.s. values of radial fluctuation velocity in the zone of establishment (ZFE)

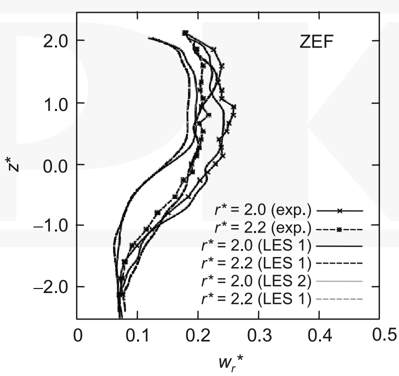

Fig. 13. Comparison of axial profiles of r.m.s. values of radial fluctuation velocity in the zone of the established flow (ZEF)

The power number P_O was calculated from impeller torque M_k which was obtained from the force balance on the impeller surface provided by the CFD calculations [7]:

$$P = 2\pi n M_k, \tag{2}$$

$$P_O = \frac{P}{\rho n^3 D^5}. \tag{3}$$

For Rushton turbine the results of the power number could be compared with the empirical correlation [21, 22], relating the power number to the relative blade thickness t/D and the relative vessel diameter T/T_0:

$$P_O = 2.512\left(\frac{t}{D}\right)^{-0.195}\left(\frac{T}{T_0}\right)^{0.063}, \tag{4}$$

where t = 2 mm is the thickness of the separating disc of a standard Rushton impeller and quantity T_0 = 1 m. The power number derived from LES 2 calculations (Eq. 3) was Po = 5.32 and it is in a good agreement with power number calculated by (Eq. 4) where Po = 5.00.

5. Conclusions

The flow in the discharge stream from the standard Rushton turbine was calculated by the Large Eddy Simulation approach. The comparison of the mean radial ensemble-averaged velocity profiles obtained from LDA measurements gives good agreement with the calculated results from both LES cases. The r.m.s values of fluctuating velocity show the similar shape of profiles, but the calculations mostly underestimated the values obtained by the LDA measurements. The ensemble-averaged results show the dependency on the spatial resolution of the calculations (mesh resolution) and on the measurement method (size of measurement volume), namely the r.m.s values of fluctuations are strongly affected by a spatial averaging. Calculated values of the root mean square difference from the mean velocities show the increasing trend from lower dimensionless radius to the value r^* = 1.8 where it probably indicates the boundary between the zone of the flow establishment and the zone of the established flow. The same trend is shown in the comparisons of the r.m.s. values of the fluctuating velocities. The power number Po = 5.32 derived from the impeller torque calculations of the presented LES numerical modeling is very close to the value Po = 5.00 estimated from empirical correlation based on experimental measurements.

This research has been subsidized by the research project No. GA CR P101/12/2274 and RVO: 67985874.

References

[1] Ben-Nun R., Sheintuch M., *Characterizing turbulent jet properties of radial discharge impeller: potential core, spreading rate and averaged flow field parameters*, 9th European Congress of Chemical Engineering, The Hague (NL), April 2013.

[2] Yeoh S., Papadakis G., Yianneskis M., *Numerical Simulation of Turbulent Flow Characteristics in a Stirred Vessel Using the LES and RANS Approaches with the Sliding/Deforming Mesh Methodology*, Chemical Engineering Research and Design, vol. 82, no. 7, 2004, pp. 834-848.

[3] Joshi J.B., Nere N.K., Rane C.V., Murthy B.N., Mathpati C.S., Patwardhan A.W., Ranade V.V., *CFD simulation of stirred tanks: Comparison of turbulence models (Part I: Radial flow impellers)*, The Canadian Journal of Chemical Engineering, vol. 89, no. 1, 2011, pp. 23-82.

[4] Joshi J.B., Nere N.K., Rane C.V., Murthy B.N., Mathpati C.S., Patwardhan A.W., Ranade V.V., *CFD simulation of stirred tanks: Comparison of turbulence models (Part II: Axial flow impellers, multiple impellers and multiphase dispersions)*, The Canadian Journal of Chemical Engineering, vol. 89, no. 4, 2011, pp. 754-816.

[5] Coroneo M., Montante G., Paglianti A., Magelli F., *CFD prediction of fluid flow and mixing in stirred tanks: Numerical issues about the RANS simulations*, Computers & Chemical Engineering, vol. 35, no. 10, 2011, pp. 1959-1968.

[6] Bakker A., Laroche R., Wang M., Calabrese R., *Sliding Mesh Simulation of Laminar Flow in Stirred Reactors*, Chemical Engineering Research and Design, vol. 75, no. 1, 1997, pp. 42-44.

[7] Gimbun J., Rielly C.D., Nagy Z.K., Derksen J.J., *Detached eddy simulation on the turbulent flow in a stirred tank*, AIChE Journal, vol. 58, no. 10, 2012, pp. 3224-3241.

[8] Derksen J., Van den Akker H., *Large eddy simulations on the flow driven by a Rushton turbine*, AIChE Journal, vol. 45, pp. 209-221, FEB 1999.

[9] Derksen J., *Long-time solids suspension simulations by means of a large-eddy approach*, Chemical Engineering Research and Design, vol. 84, JAN 2006, pp. 38-46.

[10] Bakker A., Oshinowo L., *Modelling of Turbulence in Stirred Vessels Using Large Eddy Simulation*, Chemical Engineering Research and Design, vol. 82, no. 9, 2004, pp. 1169-1178.

[11] Jahoda M., Moštěk M., Kukuková A., Machoň V., *CFD modeling of liquid homogenization in stirred tanks with one and two impellers using large eddy simulation*, Chemical Engineering Research and Design, vol. 86, 2007, pp. 616-625.

[12] Li Z., Hu M., Bao Y., Gao Z., *Particle Image Velocimetry Experiments and Large Eddy Simulations of Merging Flow Characteristics in Dual Rushton Turbine Stirred Tanks*, Industrial & Engineering Chemistry Research, vol. 51, no. 5, 2012, pp. 2438-2450.

[13] Li Z., Bao Y., Gao Z., *PIV experiments and large eddy simulations of single-loop flow fields in Rushton turbine stirred tanks*, Chemical Engineering Science, vol. 66, no. 6, 2011, pp. 1219-1231.

[14] Gillissen J.J., Van den Akker H.E., *Direct numerical simulation of the turbulent flow in a baffled tank driven by a Rushton turbine*, AIChE Journal, vol. 58, no. 12, 2012, p. 3878-3890.

[15] Kolář V., Filip P., Curev A., *Hydrodynamics of radially discharging impeller stream in agitated vessels*, Chemical Engineering Communications, vol. 27, 1984, pp. 313-326.

[16] Drbohlav J., Fořt I., Máca K., Ptáček J., *Turbulent characteristics of discharge flow from turbine impeller*, Coll. Czech. Chem. Commun., vol. 43, 1978, pp. 3148-3161.

[17] Fořt I., Möckel H. O., Drbohlav J., Hrach M., *The flow of liquid in a stream from the standard turbine impeller*, Coll. Czech. Chem. Commun., vol. 44, 1979, pp. 700-710.

[18] Obeid A., Fořt I., Bertrand J., *Hydrodynamic characteristics of flow in systems with turbine impeller*, Coll. Czech. Chem. Commun., 48, 1983, p. 568-577.

[19] Talaga J., Fořt I., *The velocity field in the discharge stream from a rushton turbine impeller*, 14th European Conference on Mixing, Warszava, 10–13 September 2012.
[20] Venneker B.C., Derksen J.J., Van den Akker H.E.A., *Turbulent flow of shear-thinning liquids in stirred tanks - The effects of Reynolds number and flow index*, Chemical Engineering Research and Design, vol. 88(7), 2010, pp. 827-843.
[21] Bujalski W., Nienow A.W., Chatwin S., Cooke M., *The dependency on scale of power numbers of Rushton disk turbine*, Chemical Engineering Science, vol. 42(2), 1987, pp. 317-326.
[22] Beshay K.R., Kratěna J., Fořt I., Brůha O., *Power Input of High-Speed Rotary Impellers*, Acta Polytechnica, vol. 41, no. 6, 2001, pp. 18-23.